Cement & Concrete Composites 39 (2013) 82–92

Contents lists available at SciVerse ScienceDirect

Cement & Concrete Composites

journal homepage: www.elsevier.com/locate/cemconcomp

Hydration kinetics in hybrid binders: Early reaction stages

I. Garcia-Lodeiro *, A. Fernandez-Jimenez, A. Palomo

Instituto Eduardo Torroja (IETcc, CSIC), C/Serrano Galvache 4, 28033 Madrid, Spain

ARTICLE INFO

Article history:
Received 25 December 2012
Received in revised form 21 March 2013
Accepted 24 March 2013
Available online 6 April 2013

Keywords:
Hybrid cements
Calorimetry
Geopolymer
Model
Composite

ABSTRACT

Activated blends of Portland cement and fly ash with a high ash content (>70%) are a new alternative to traditional OPCs. A number of papers have been published on C–S–H and N–A–S–H, the two gels that constitute the main cementitious products generated by the alkaline activation of these cements, and the elements that may be taken up into their structure. Very little is known about the kinetics of these systems, however, particularly during the early stages of the reaction. The present study used isothermal conduction calorimetry to explore hydration kinetics during the first 72 h in a cement containing 30% OPC and 70% fly ash. Two activating solutions were used: a mix of NaOH + Na_2SiO_3 and a Na_2CO_3 solution. The findings showed that hydration kinetics were substantially modified by the type of alkaline activator used, particularly with respect to the secondary phases generated. In both cases the main reaction product appeared to be a mix of C–A–S–H and (N,C)–A–S–H gels, whose proportions were clearly impacted by the type of activator used.

1. Introduction

The ultimate aim of research into the alkaline activation of aluminosilicates, a line of study that has been consolidated in recent years, is to determine the viability of binders other than ordinary Portland cement (OPC). The key differences between alkali-activated systems, which are based on the reactivity of silico-aluminous materials, and conventional Portland cement systems are the absence of lime in the mix and the high alkalinity required to trigger the activation reactions [1,2]. The result is the formation of different reaction products. The product of OPC hydration is a calcium silicate hydrate (C–S–H gel) [3,4], whereas the main product generated during the alkaline activation of silico-aluminous materials is an alkaline aluminosilicate known as N–A–S–H gel [5,6].

The activation of Portland cement blends containing high proportions of fly ash is a promising alternative for the construction binder industry. The reaction products obtained, C–S–H and N–A–S–H gels, and their compatibility, however, have yet to be explored in depth. The literature contains some initial indications of the properties of the products formed. Yip et al. [7], for instance, reported that two types of gels co-exist in alkali-activated metakaolin and slag blends: a C–S–H gel with Al in its composition and a silicoaluminous gel containing some calcium. The presence of two types of gels, C–S–H and N–A–S–H, was also observed by Palomo et al. in the alkaline activation of two systems: blends of metakaolin and $Ca(OH)_2$ on the one hand [8] and fly ash and Portland cement clinker on the other [9]. Co-precipitation of the two types of gels has been confirmed in such systems. They do not precipitate as pure gels, however, but are affected by the presence of other elements: C–S–H gel takes up aluminium (C–A–S–H gel) [10] and calcium partially replaces sodium in N–A–S–H gel ((N,C)–A–S–H gel) [11]. The type and characteristics of the gel formed are clearly conditioned by the working pH and the calcium concentration in the system; a high calcium content and pH level favour C–A–S–H over N–A–S–H gel formation [12]. Nonetheless, little is known about the kinetics of the reactions taking place during the alkaline activation of this type of hybrid systems, particularly in the early stages.

Isothermal conduction calorimetry, a technique that monitors heat flow and cumulative heat over time in chemical (here hydration) reactions, is an effective method for studying cement system hydration kinetics [13]. It was used in the present study to explore hydration kinetics during the first 72 h in alkali-activated blends containing 30% OPC and 70% fly ash.

2. Experimental

2.1. Materials

The prime materials used in this study were a commercial 52.5 NSR Portland cement and a type F fly ash (ASTM C618-03) [14]) supplied by a Spanish coal-fired steam plant. The chemical composition of these two materials is given in Table 1.

2.2. Methodology

Early hydration stage heat flow and cumulative heat were determined at a constant 25 °C on a THERMOMETRIC TAM Air

* Corresponding author. Tel.: +34 913020440x253; fax: +34 913020700.
E-mail address: iglodeiro@ietcc.csic.es (I. Garcia-Lodeiro).

0958-9465/$ - see front matter © 2013 Elsevier Ltd. All rights reserved.
http://dx.doi.org/10.1016/j.cemconcomp.2013.03.025

Table 1
Chemical composition of the starting materials (wt.%).

	SiO_2	CaO	Al_2O_3	Fe_2O_3	MgO	SO_3	Na_2O_{eq} [c]	Other	LoI [d]	I.R. [e]
OPC [a]	20.26	62.79	6.33	2.30	0.18	2.82	0.75	–	2.56	0.73
FA [b]	54.32	3.11	25.22	7.01	1.69	0.01	2.47	3.46	2.09	0.66

[a] Portland cement.
[b] Fly ash.
[c] Na_2O_{eq} wt.% $Na_2O + 0.658\ K_2O$ wt.%.
[d] Loss on ignition.
[e] Insoluble residue.

isothermal conduction calorimeter. The test samples (solids) were weighed and uniformly distributed in vials. The water or activator solutions were weighed in a syringe. Five-gram solid samples were used, with a liquid:solid ratio of 0.35. The calibration baseline was established by recording the heat flow for ground quartz mixed in water with the same liquid:solid ratio.

The systems studied consisted of a 70/30 (wt) fly ash/cement blend (M), hydrated with water or an alkali solution. The control systems consisted of 100% water-hydrated or alkali-activated Portland cement pastes (OPC) or 100% fly ash (FA) alkaline activated at ambient temperature (25 °C).

Prior to insertion in the calorimeter, the pastes were prepared with deionised water (W) or one of two alkaline solutions: a 12.5-M mix of NaOH and sodium silicate (solution D1) (pH = 13.25, $\rho \cong 1.2$) or a 2-M Na_2CO_3 solution (solution D2) (pH = 11.6, $\rho \cong 1.1$).

The pastes were mixed by hand for 3 min prior to insertion in the calorimeter. While ideally the kinetic study should commence as soon as the solid blends come into contact with the solutions, satisfactory preparation of the sample prior to pouring it into the calorimeter is essential and the loss of information during this short initial period of time, inevitable. Since the first peak recorded on the calorimetric curves (commonly associated with the dissolution of the material) is unreliable, it has been omitted from the present discussion. All the samples were removed from the calorimeter 120 h after mixing.

The fly ash/cement blends (M) activated with the alkaline solutions (D1 and D2) were analysed with XRD and FTIR at different ages, beginning a few minutes after initial mixing through 7 days. Selected samples were also analysed with BSEM/EDX techniques. The ages studied for each binder (MD1 and MD2) were chosen on the grounds of the information provided by the calorimetric curves. XRD and FTIR analyses were conducted on the control samples at ages likewise determined on the grounds of the calorimetric profiles.

X-ray diffractograms of powdered samples were recorded on a 40-kV, 50-mA Phillips PW 1730 Cu Ka diffractometer. Specimens were step-scanned at 2° min^{-1}, with 2Θ in the 2–60° range, a 1° divergence slit, a 1° anti-scatter slit and a 0.1-mm receiving slit. The FTIR spectra were obtained on an ATIMATT-SON FTIR-TM series spectrophotometer from specimens prepared by mixing 1 mg of sample with 300 mg of KBr. Spectral analysis was performed at a resolution of 4 cm^{-1} over the 4000–400 cm^{-1} range. Finally, polished sections of selected samples were carbon-coated and studied under a JEOL JSM scanning electron microscope fitted with a solid-state BSE detector and a LINK-ISIS energy dispersive X-ray (EDX) analyser.

3. Results

3.1. Calorimetric studies

The heat flow (in J/g h) profiles and cumulative heat (J/g) vs time graphs for the pastes prepared with the three hydration liquids (W, D1 and D2) are shown in Fig. 1, where three periods can be identified: period I (prior to when the main peak was recorded), period II (in which the main peak was recorded) and period III (after the main peak was recorded). Table 2, in turn, lists the peak heights and times in the second period, as well as the cumulative heat after 120 h for all the pastes studied. The findings are described below.

3.1.1. Water-hydrated systems (W)

The calorimetric curve for the OPCW paste followed a pattern characteristic of the hydration curves for Portland cements [13] (Fig. 1a). The period II peak, with a maximum at 5.70 h and a shape likewise characteristic of Portland cement hydration [13], was associated with the alite reaction and consequently with reaction product (mainly C–S–H gel and portlandite) precipitation.

The water-hydrated 100% FA system (FAW) exhibited no heat exchange (cumulative heat curve, Fig. 1b): i.e., when hydrated with water at ambient temperature, the ash was apparently inert, with no intrinsic hydraulic properties.

The system consisting of 70% FA + 30% OPC hydrated with water (MW) generated heat flow and total heat curves very similar to the Portland control (OPCW) curves (Fig. 1a and b), although certain differences were observed. The peak in period II was less intense than the same peak in OPCW, and shifted to later hydration times (8.94 h), while the cumulative heat value was around 3.3 times lower (Fig. 1b and Table 2). Both the lower peak height and the lesser amount of cumulative heat can be explained by the dilution effect [15,16]: the amount of cement available was substantially smaller in the MW than in the OPCW system (100% OPC), given that in the conditions prevailing in the latter, the ash was inert or scantly reactive.

3.1.2. Systems activated with solution D1($NaOH + Na_2SiO_3$, pH 13.5)

The general shape of the heat flow profile for system OPCD1 (100% OPC) (Fig. 1c) differed considerably from the curve observed for the water-hydrated system (OPCW) (Fig. 1a); the presence of alkalis in the medium lowered the intensity of the peak (period II) by nearly 85% (Fig. 1c and Table 2). These findings, which support earlier evidence of high alkali content-induced delays in normal Portland cement hydration [17–19], was in turn confirmed by the cumulative heat curves (see Fig. 1d). OPCD1 released on the order of twofold less cumulative heat than the same cement when hydrated with water (OPCW) (Table 2).

The general shape of the heat flow curve for system FAD1 (100% FA) (Fig. 1c) was similar to the profile for the water-hydrated fly ash (FAW) (Fig. 1a). No calorimetric peak that could be associated with the precipitation of reaction product was observed at any time during the trial, however. Although the presence of alkalis induced some degree of ash dissolution, this process is very slow at ambient temperature, and too little N–A–S–H gel precipitated to be detected. Precipitation of this kind of gel usually calls for higher temperatures [5,6]. At ambient temperature, the ash neither set nor hardened in a technologically viable time frame.

The calorimetric curve for the main object of this study, the fly ash/cement blend activated with solution D1 (MD1), showed a

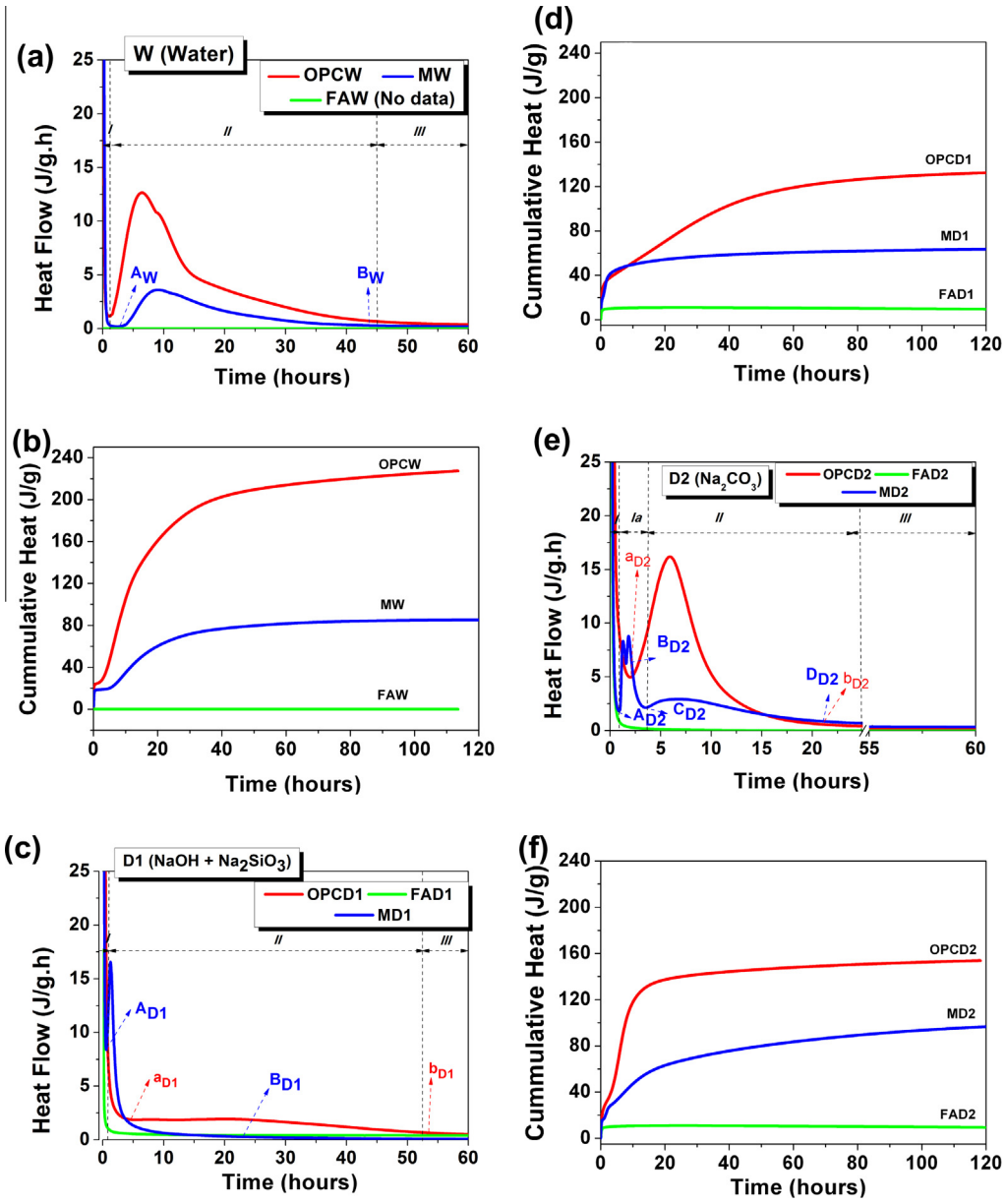

Fig. 1. Heat flow and cumulative heat of OPC, FA and M systems hydrated with (a) and (b) W (water); (c) and (d) D1 ($NaOH + Na_2SiO_3$); (e) and (f) D2 (Na_2CO_3).

Table 2
Summary of calorimetric characteristics of the systems studied.

Sample	Activator	Period				Total heat After 120 h (J/g)
		Period Ia		Period II		
		Peak eight (J/g h)	Time (h)	Peak height (J/g h)	Time (h)	
OPC	W	–	–	12.73	5.70	226.99
	D1	–	–	1.97	21.79	131.55
	D2	–	–	16.20	5.70	153.24
FA	D1	–	–	–	–	–
	D2	–	–	–	–	9.47
M	W	–	–	3.66	8.94	85.12
	D1	–	–	16.55	1.26	63.42
	D2	8.23	1.26	2.93	6.41	96.41
		8.82	1.84			

very narrow signal with a peak intensity of 16.55 J/g h at 1.36 h (period II) (Table 2). This signal would suggest that the presence of alkalis induced synergies between the ash and the cement, as discussed in a later section of this paper.

Another significant characteristic of the materials activated with solution D1 was revealed by the cumulative heat curves (Fig. 1d). While during the early hours of the reaction, more cumulative heat was released by MD1 than by OPCD1, at later ages (over

20 h) the latter continued to release heat, whereas the process had obviously concluded in the MD1 blend.

3.1.3. Systems activated with solution D2 (Na_2CO_3, pH 11.6)

When the OPC was activated with solution D2 (with a lower pH than D1), the features of its calorimetric curve (Fig. 1e) and the curve for water-hydrated cement, OPCW (Fig. 1a), were fairly comparable. The OPCD2 curve had a peak in period II at practically the same time (5.70 h) as observed for OPCW, although less cumulative heat was released.

The calorimetric curve for FAD2 (Fig. 1e) was practically the same as obtained with activator D1 (Fig. 1c): no peak was detected that could be associated with any reaction, while the cumulative heat profile indicated no heat exchange whatsoever.

The heat flow curve (Fig. 1e) for MD2 was very different from the curves obtained for the water-(MW) and solution D1-hydrated (MD1) systems (Fig. 1c). In this case, a signal with two peaks at 1.26 and 1.84 h appeared in a period denominated *Ia*. The presence of this double peak would obviously have to be associated with the system activator (Na_2CO_3 solution). The period II peak (t = 6.41 h), normally associated with the precipitation of reaction products, was slightly retarded and lower in height than on the OPCD2 profile, possibly denoting a delay in activation/hydration.

The cumulative heat curves revealed other pertinent findings (Fig. 1f). Reference system OPCD2 and the water-hydrated system (OPCW) exhibited behaviour similar, although cumulative heat was on the order of 1.5 times lower in the former. Here also, the high alkalinity of the medium was observed to retard cement hydration. In contrast, cumulative heat followed a different pattern in MD2 than observed in MW (Fig. 1b): the early hours were characterised by steeper exponential growth, denoting rapid heat release during the precipitation of the first reaction products. After 24 h, however, both curves (MW and MD2) were nearly flat, an indication of scant heat release.

3.2. Mineralogical study at short reaction times

XRD and FTIR analyses were conducted on pastes MD1 and MD2 and the control samples (alkali-activated 100% OPC and water-hydrated fly ash/cement blend (M)) to ascertain the nature of the reaction products formed. Water-hydrated OPCW and FAW were not analysed because sufficient information on their mineralogy is available in the literature [3,20–23]. The systems consisting of alkali-activated 100% FA (FAD1 and FAD2) prepared at 25 °C were not characterised either, for under these conditions the ash neither set nor hardened within the established reaction times; i.e., barely any reaction took place [24].

The ages at which the pastes were studied were determined on the grounds of their respective calorimetric profiles: the points at which the analyses were conducted are labelled in Fig. 1a (A_w and B_w (in system MW)), Fig. 1c (A_{D1} and B_{D1} (in system MD1); a_{D1} and b_{D1} (in system OPCD1)) and Fig. 1d (A_{D2}, B_{D2}, C_{D2} and D_{D2} (in system MD2); a_{D2} and b_{D2} (in system OPCD2)). The 7-day samples were likewise analysed. Table 3 summarises the "mineralogical moments" selected on the grounds of the calorimetric curves for the pastes. (A "mineralogical moment" reflects the mineralogy of a substance at a given time, constituting a snapshot of the mineral composition of the material studied.)

3.2.1. Water-hydrated systems

Fig. 2a and b respectively show the diffraction patterns and FTIR spectra for the water-hydrated blend (70% FA + 30% OPC). The 45-h diffractograms exhibited a significant decline in the anhydrous cement phases (alite and belite). New peaks were observed and associated with portlandite and ettringite (typical secondary products in OPC hydration) [3]. In contrast, the crystalline quartz and mullite phases present in the ash [21,25] remained unaltered. These findings were compatible with the existence of blended cement hydration as described in the literature [26].

Since C–S–H gel, the main Portland cement hydration product, is amorphous to X-rays [3], FTIR was used to detect its presence or otherwise. The greatest changes in the FTIR spectra for the blend were observed from 45 h onward. In addition to the bands at 1100 cm^{-1} and 1050 cm^{-1}, respectively associated with the symmetrical stretching vibrations generated by the Si–O–Si bonds in quartz [27] and anhydrous fly ash [21,28], a shoulder was observed at 998 cm^{-1}. As this frequency was too high to be attributed to a typical C–S–H gel (normally detected at around 970 cm^{-1}) [22,23,29,30], the band may have been generated by a silicon-rich gel whose origin was not elucidated in this study. In the 7-day spectra, this shoulder shifted to 973 cm^{-1}, a frequency characteristic of C–S–H gel vibration.

3.2.2. Systems alkali-activated with D1

Fig. 3a and b shows the diffraction patterns and FTIR spectra for the 100% cement system (OPC) activated with solution D1 ($NaOH + Na_2SiO_3$) (OPCD1). The diffraction lines for alite and belite, the phases found in anhydrous cement, remained fairly intense even after 7 days of activation. This finding may be indicative of a delay in the hydration reactions in this highly alkaline system compared to normal OPC hydration [18,19]. No ettringite was detected. Signals associated with portlandite and calcite precipitation were observed at 3.9 h; while initially low, their intensity rose with activation time (59 h and 7 days).

A comparison of the FTIR spectra for the activated and anhydrous samples (Fig. 3b) clearly revealed that activation had taken place after 59 h, when the band located at 930 cm^{-1} associated with alite (ν_{as} Si–O–Si stretching vibrations in C_2S [29,30]) shifted to 984 cm^{-1}. Its 7-day position at 970 cm^{-1} was attributed to the asymmetric stretching vibrations generated by the ν_{as} Si–O–Si bonds in C–S–H gel. The band located at 984 cm^{-1} may be associated with the formation of silicon-richer and consequently more

Table 3
Characterisation times.

Sample	Calorimetric period	Analysis point	Mineralogical moment	Sample	Calorimetric period	Analysis point	Mineralogical moment
MD1	II	A_{D1}	34 min	OPCD1	II	a_{D1}	3.9 h
		B_{D1}[a]	24 h			b_{D1}	59 h
	III	C_{D1}	7 days		III	c_{D1}	7 days
MD2	Ia	A_{D2}	53 min	OPCD2	II	a_{D1}	2.0 h
		B_{D2}	1.37 h			b_{D1}	24 h
		C_{D2}	3.32 h		III	c_{D1}	7 days
	II	D_{D2}[a]	24 h	MW	II	Aw	2.74 h
	III	E_{D2}	7 days			B_W[a]	45 h
					III	C_W	7 days

[a] Samples selected to be analysed by BSEM/EDX.

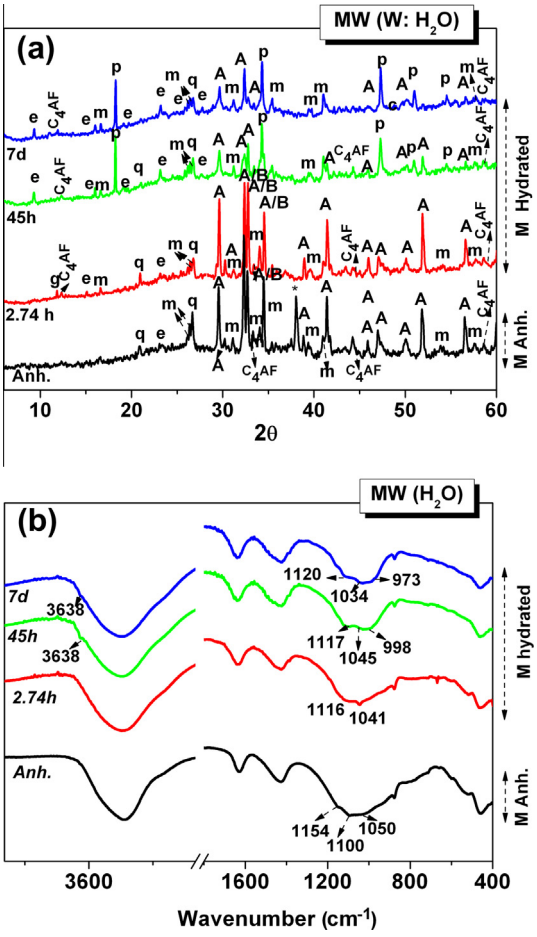

Fig. 2. (a) XRD patterns and (b) FTIR spectra of MW at the mineralogical moments listed in Table 3 (Legend: A: $3CaO{\cdot}SiO_2$; B: $2CaO{\cdot}SiO_2$; C_4AF, ferrite phase; p: portlandite; c, calcite ($CaCO_3$); G, gaylussite ($Na_2Ca(CO_3)_2{\cdot}5H_2O$); q, quartz ($SiO_2$); m, mullite ($3Al_2O_3{\cdot}2SiO_2$); e: ettringite ($3CaO{\cdot}Al_2O_3{\cdot}3CaSO_4{\cdot}3H_2O$).

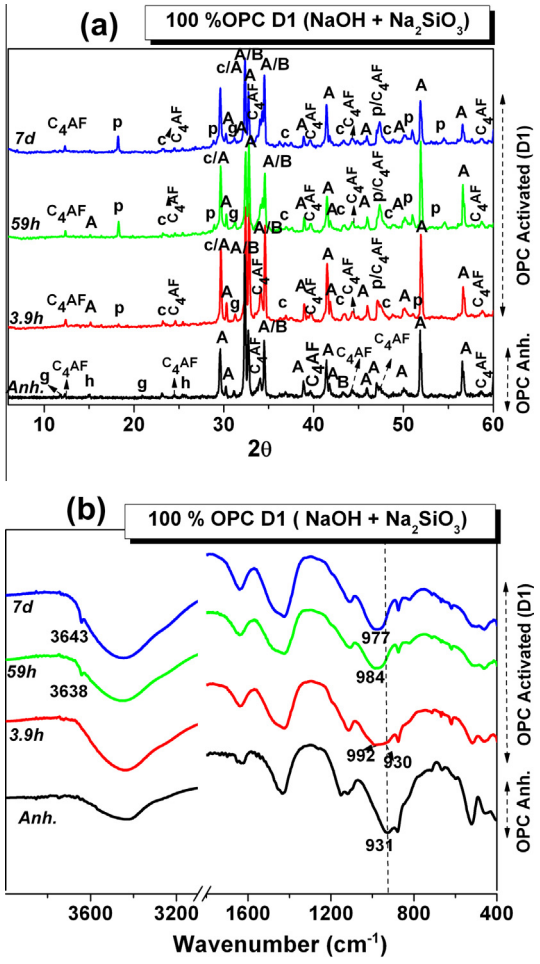

Fig. 3. (a) XRD patterns and (b) FTIR spectra of OPCD1 at the mineralogical moments listed in Table 3 (Legend: A: $3CaO{\cdot}SiO_2$; B: $2CaO{\cdot}SiO_2$; g: Gypsum ($Ca_2SO_4{\cdot}2H_2O$); h: $CaSO_4{\cdot}1/2H_2O$; C_4AF, ferrite phase; p: portlandite $Ca(OH)_2$; c, calcite ($CaCO_3$); q, quartz (SiO_2); m, mullite ($3Al_2O_3{\cdot}2SiO_2$).

polymerised gels induced by the soluble silica added with the activator [31].

The shoulder at 990 cm^{-1} appearing after 3.9 h was associated with anhydrous belite (ν_{as} Si–O–Si). The presence of portlandite was confirmed by the presence of a band at around 3640 cm^{-1} attributed to O–H group asymmetric stretching vibrations [22,23].

The findings for system MD1 (see Fig. 4) were revealing. The 34-min XRD pattern for MD1 (Fig. 4a) differed from the diffractogram for the anhydrous material: in addition to the signals for the inert ash phases (quartz and mullite), it exhibited a series of diffraction lines associated with calcite precipitation. The intensity of the lines generated by the cement anhydrous phases (C_3S and C_4AF) declined only slightly until the 7th day, when a substantial difference was observed. This latter finding confirmed that the presence of alkalis retarded cement hydration. In addition, a halo normally attributed to the precipitation of an amorphous product appeared at 25–40 2Θ. No portlandite was detected either in the early age or the 7-day material.

As mentioned above, both the C–S–H gel, the main Portland cement hydration product, and N–A–S–H gel, the main product of fly ash alkaline activation, are X-ray amorphous [2,3,6]. Their possible presence in the pastes was therefore studied with FTIR (Fig. 4b). The main band located at 1050 cm^{-1} in the 34-min spectrum for the anhydrous material and associated with the ν_{as} generated by the T–O (T:Si or Al) bonds in the fly ash [19] shifted to significantly lower frequencies (1010 cm^{-1}) in the spectra for the pastes. This shift in the main ash band may have been associated with the dissolution of its vitreous component. Moreover, in the 24-h spectra, this band was observed to shift to even shorter wavelengths that lie within the vibration range for N–A–S–H-like gels [23,28].

On the 7-day FTIR spectrum, the main band for the activated blend was centred on ν_{as} 963 cm^{-1}, i.e., Si–O–Si vibration frequency values characteristic of C–S–H/C–A–S–H gel [22,23].

3.2.3. Systems alkali-activated with D2

Activating OPC with solution D2 (Na_2CO_3) (OPCD2) (see Fig. 5a) led to findings very similar to the results observed for system D1 (system OPCD1) (Fig. 3a). Here also, the XRD pattern for the activated samples exhibited a series of lines associated with portlandite and calcium carbonate. The intensity of the lines attributed to this latter phase was greater than observed in the preceding system (OPCD1). This was to be expected in light of the presence in this sample of CO_3^{2-} ions, which formed part of the activator. The height of the lines attributed to the anhydrous phases declined more steeply than in system D1. No signals associated with ettringite were detected here, either.

The most prominent difference between the FTIR spectra for this and the anhydrous sample was observed after 7 days, when the band at 930 cm^{-1} (C_3S) [29,30] shifted to 970 cm^{-1} (C–S–H gel) [22,23]. Nonetheless, the shoulder at 990 cm^{-1} associated with C_2S [30] was not detected at this hydration time. The band at 3640 cm^{-1} [22,23] confirmed the presence of portlandite ($Ca(OH)_2$) here also.

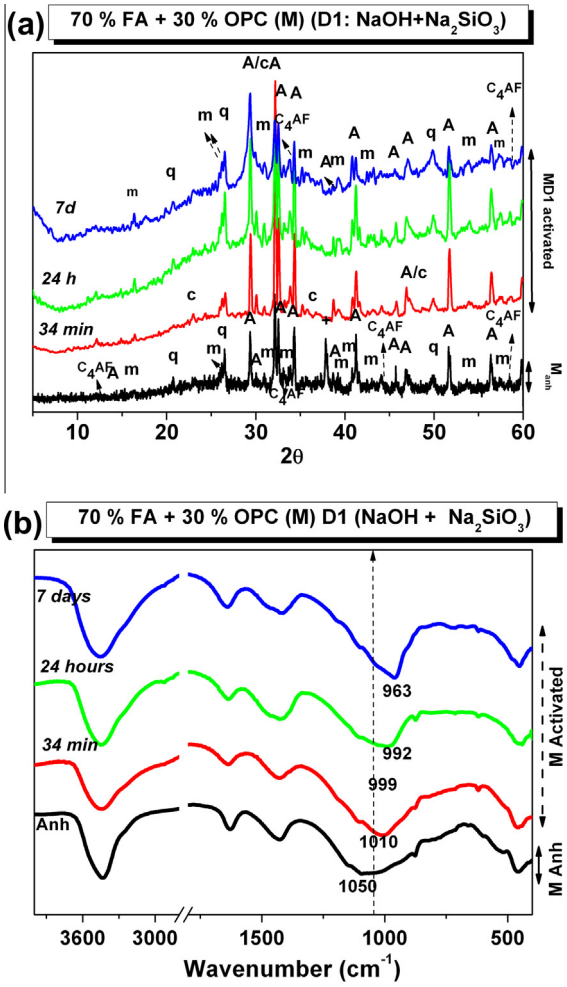

Fig. 4. (a) XRD patterns and (b) FTIR spectra of the MD1 (70% FA + 30% OPC) activated with solution D1 at the mineralogical moments listed in Table 3 (Legend: q, quartz (SiO_2); c, calcite ($CaCO_3$); m, mullite ($3Al_2O_3{\cdot}2SiO_2$); A, $3CaO{\cdot}SiO_2$; C_4AF, ferrite phase).

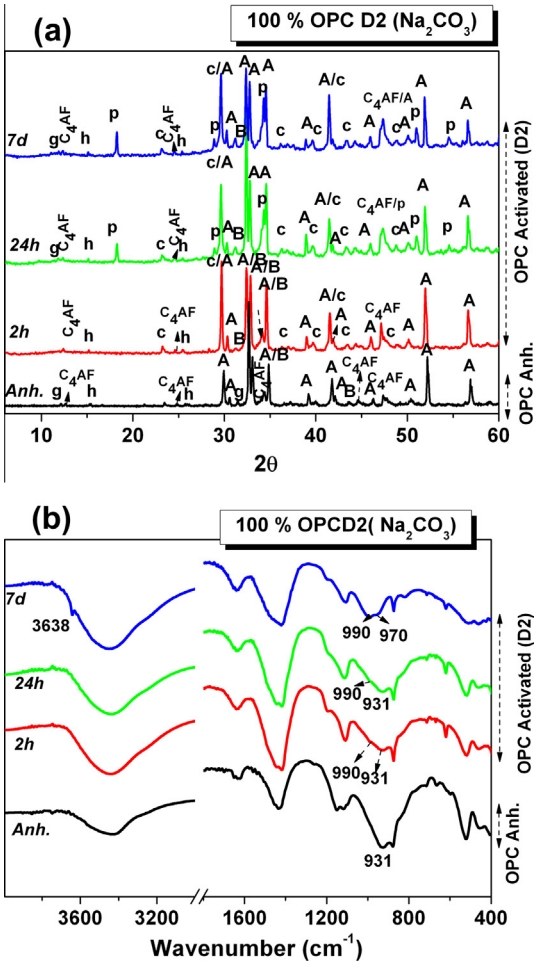

Fig. 5. (a) XRD patterns and (b) FTIR spectra of OPCD2 at the mineralogical moments listed in Table 3 (Legend: A: $3CaO{\cdot}SiO_2$; B: $2CaO{\cdot}SiO_2$; g: Gypsum ($Ca_2SO_4{\cdot}2H_2O$); h: $CaSO_4{\cdot}1/2H_2O$; C_4AF, ferrite phase; p: portlandite $Ca(OH)_2$; c, calcite ($CaCO_3$); q, quartz (SiO_2); m, mullite ($3Al_2O_3{\cdot}2SiO_2$).

When activated with solution D2 (Na_2CO_3), blended system M generated XRD patterns that differed substantially from the diffractograms for the same system when hydrated with solution D1 (MD1). In addition to the diffraction lines associated with calcite, the early age (52.8-min) diffractograms (Fig. 6a) contained a series of signals associated with a sodium–calcium carbonate known as gaylussite, whose presence was reported in earlier studies on Na_2CO_3-activated Portland cement systems [18,19]. Not unexpectedly, the diffraction lines associated with this phase disappeared in the 7-day pattern, for when gaylussite dissolves it normally forms calcite [32]. The diffractograms also exhibited a small halo at 20–40 2Θ, associated with the precipitation of an amorphous reaction product.

The lines associated with anhydrous cement phases (mainly C_3S) failed to show any significant changes until the 7th day, when their height declined substantially to levels considerably lower than observed for the 7-day lines for system D1. This confirmed that while the hydration reactions induced by D2 proceeded slowly at first, this activator hydrated the cement phases more effectively than D1 due to its lower alkalinity. Moreover, the 7-day patterns contained diffraction lines attributed to hemi- and monocarboaluminates (AF_m phases) not detected in system MD1. Such species normally precipitate jointly with C–A–S–H gel [10,33,34].

No lines associated with $Ca(OH)_2$ were observed at any age, although this phase was detected in the 7-day FTIR spectra (Fig. 6b), an indication that it probably adopted the form of nanocrystalline or poorly crystallised portlandite [10]. The possibility of sample interaction with the atmospheric CO_2 and concomitant carbonation cannot be ruled out, however, for the pastes were exposed to the laboratory air.

The FTIR (Fig. 6b) spectra recorded for MD2 were similar to the findings for MD1. The main band on the 53-min spectrum appeared at a lower frequency (1027 cm^{-1}) than observed for the anhydrous material. Moreover, this shift intensified with reaction time up to 3.23 h, when the peak was centred at around 1010 cm^{-1}, a vibration frequency characteristic of N–A–S–H type gels [28].

On the 7-day spectrum, the band shifted to a vibration frequency of 967 cm^{-1}, more characteristic of C–S–H/C–A–S–H type gels [3,10]. Moreover, a small shoulder at around 3670 cm^{-1} was attributed to the asymmetrical stretching vibrations generated by the H O H bonds in portlandite [3,10].

4. Discussion

Conduction calorimetry, a technique for studying the kinetics of chemical reactions, has always played an important role in the interpretation of mechanisms that govern Portland cement hydration. Furthermore, since this technique has contributed to a fuller understanding of the effects of supplementary cementitious mate-

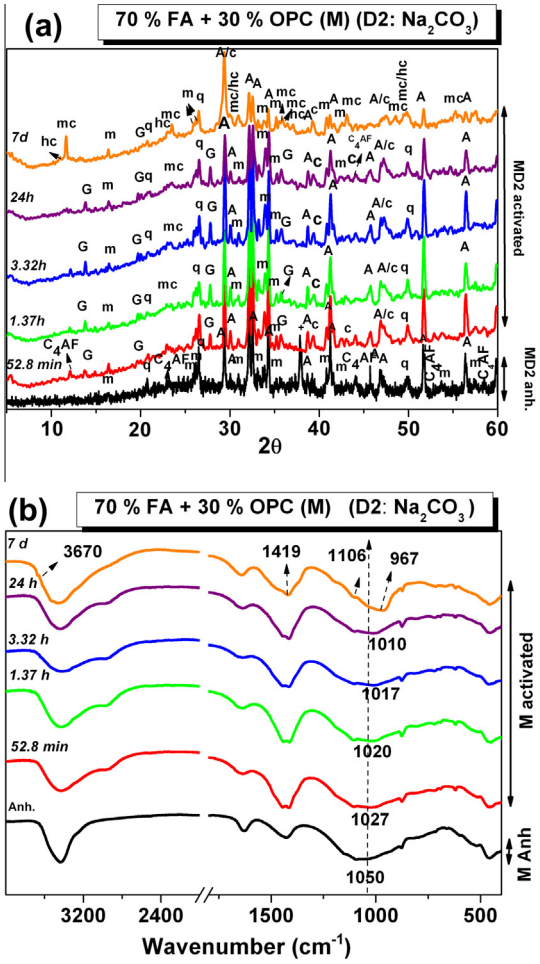

Fig. 6. (a) XRD patterns and (b) FTIR spectra for the MD2 (70% FA + 30% OPC) activated with solution D2 (Na_2CO_3) at the mineralogical moments listed in Table 3 (Legend: q, quartz (SiO_2); c, calcite ($CaCO_3$); m, mullite ($3Al_2O_32SiO_2$); A, 3CaO.SiO2, C_4AF: ferrite phase; G, gaylussite ($Na_2Ca(CO_3)_2{\cdot}5H_2O$); mc, monocarboaluminate ($Ca_4Al_2CO_3{\cdot}11H_2O$); hc, hemicarboaluminate ($Ca_4Al_2O_6(CO_3)_{0.5}(OH)11.5H_2O$)).

rials (SCMs) on hydration [13,14,35–41], it was deemed to be able to likewise contribute significantly to the study of hybrid cements. The alkaline hydration of the materials described in this paper are analysed in depth below.

4.1. Water-hydrated systems

The processes involved in OPC hydration have been more frequently explored [3]: the anhydrous clinker phases hydrate at various rates, forming C–S–H, portlandite, ettringite and AFm as the main hydrates. Blending SCMs such as FA with OPC leads to a more complex system, however, in which OPC hydration and SCM reactions occur simultaneously, with each affecting the reactivity of the other. Many examples of the effect of replacement of Portland cement with fly ash on both the products formed and on reaction kinetics can be found in the literature [37,38,40–47]. As a general rule, the use of silicon-rich SCMs induces (i) a decline in portlandite content and (ii) a decline in the Ca/Si ratio of C–S–H gel. Their use also leads to a greater uptake of aluminium in C–S–H gels. While the replacement rates applied in most of the studies cited above were not as high as in the present research (70% FA), the reaction products identified when the present blend (70% FA + 30% OPC) was hydrated with water concurred with previous findings, as described in an earlier section of this paper.

Briefly, Portland cement hydration kinetics are indisputably affected by the presence of large proportions of fly ash. The results for the MW samples revealed that hydration was retarded and considerably less heat was released than in the OPCW material (see Fig. 1b). These observations concur with the findings reported by Snelson et al. [36] for Portland–metakaolin–fly ash blends. These authors observed that during the early hours (from 1 to 18) of hydration, the ash induced a significant reduction in hydration due to the combined effects of scant pozzolanic activity and dilution. The ash–portlandite–water system reacted very slowly given the low solubility of the vitreous aluminosilicates in the moderately alkaline medium generated by Portland cement hydration [36]. Since the ash acted as a scantly reactive component in the early stages of cement hydration, the amount of water associated with its "hypothetical" hydration remained available to hydrate the cement. According to the literature, heat flow in the early stages of cement hydration is highly sensitive to the water/cement ratio and rises significantly with the ratio up to a certain value [36]. In the Snelson et al. study, inasmuch as the pozzolanic reaction attributable to the ash was negligible in the following 100 h, its only effect was to dilute the cement [40]. The cumulative heat value was observed to be inversely proportional to the ash content.

4.2. Systems alkali-activated with D1 and D2

When the materials studied here were mixed with alkaline solutions D1 and D2, and particularly with the former (which had a higher pH and alkali content), hydration differed from the patterns observed in normal water-based hydration in OPC, at least as far as reaction kinetics are concerned. The literature is divided over the effect of alkalis on cement hydration [17–19,48–54]. While some papers show that the addition of moderate concentrations of NaOH accelerates the reaction, especially in the early stages [49,51,53], others report that alkalis induce some acceleration in early age hydration but subsequently retard the reaction [50,52]. When high concentrations of alkalis are used, however, the process is clearly retarded [17–19,48], affecting not only reaction kinetics but also the amount of hydration product formed. The primary difference, then, lies in the alkaline concentration, as clearly shown here by the findings for the 100% OPC pastes prepared with the two activators. While the use of D1 (pH = 13.25) clearly retarded the reaction (see Fig. 1a and Table 2), when D2 (pH = 11.6) was applied, no material difference was observed between the resulting precipitation peak and the peak for water-hydrated paste (OPCW), in terms of either the time when the maximum was reached (stage II) or the shape of the profile.

Alkali-activated binder M (the main target of this study), which had a high ash content (70% FA + 30% OPC), behaved very differently from the water hydrated blend (MW) and the water-hydrated and alkali-activated control systems (Fig. 1). The 24-h activated MD1 and MD2 materials were characterised with BSEM/EDX to analyse the main reaction products and confirm the findings observed with other techniques (Fig. 7a and b, respectively). The analysis of blend MD1 revealed that it contained large amounts of unreacted ash and anhydrous cement particles (C_3S), along with two cementitious gels with different compositions: a C–S–H-like gel containing aluminium and small amounts of sodium (point 1, gel (N)–C–A–S–H) and a gel with a high silicon and aluminium content and smaller amounts of calcium and sodium, which the authors believe may be a N–A–S–H gel containing a certain amount of calcium ((N,C)–A–S–H [point 2]) [11,26]. The analysis of Na_2CO_3-activated paste MD2 further confirmed the presence of both types of gels, but in this case the majority product was a C–A–S–H-like gel with small amounts of sodium (point 3, (N)–C–A–S–H). The proportion of the silica- and alumina-rich gel, which here also contained some calcium (point 4, (N,C)–A–S–H)),

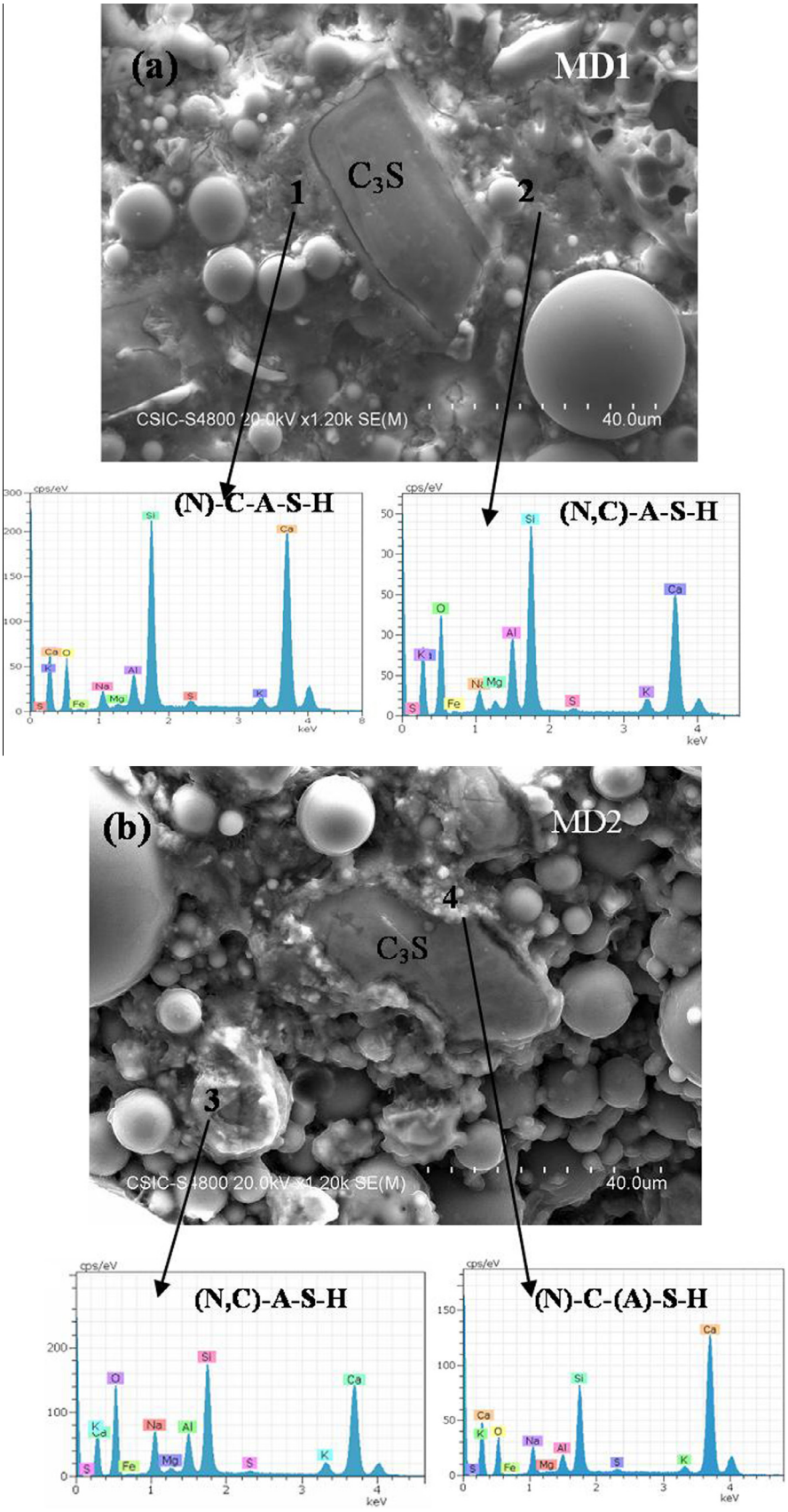

Fig. 7. BSEM/EDX analyses of (a) MD1 (24 h) and (c) MD2 (24 h).

was much smaller. In other words, the nature of the alkaline activator played an important role not only in hydration kinetics, but also in the proportion of reaction product precipitating.

On the grounds of the XRD, FTIR and BSEM/EDX characterisation of MD1 and MD2 at the "mineralogical moments" defined earlier, a model can be put forward to interpret the possible reactions taking place and the formation of reaction products in the early stages of hydration, depending on the activator used. A flow diagram for the model is shown in Fig. 8.

The presence of alkalis reduced cement dissolution slightly but expedited fly ash dissolution, which was further favoured by the heat released during the dissolution of the anhydrous phases of the cement. For that reason both the reaction in the alkali-activated systems containing 100% ash (FAD1 and FAD2) and ash reactivity in the presence of cement without alkalis (system MW) were practically nil. In other words, both alkalis and an initial source of heat (OPC hydration reactions) are required to expedite the initial reaction of the fly ash. This hypothesis is supported by the FTIR findings. The spectrum for the anhydrous blend contained a band associated with the asymmetric bending vibrations generated by the T–O bond at 1050 cm^{-1}. This signal shifted to clearly lower frequencies on the spectra for the hydrated material (1010 cm^{-1} for 34-min MD1 and 1027 cm^{-1} for 52.8-min MD2, Figs. 4b and 6b).

The decline in the intensity of the diffraction lines associated with the anhydrous phases of the cement (Figs. 4a and 6a) also confirmed the initial dissolution of the cement and ash. After period I, binder M hydration clearly differed with the alkaline activator used (Fig. 8), because both the initial conditions and the chemical species deriving from the activator varied.

In material MD1 (in which the activator was a mix of NaOH + -sodium silicate, pH = 13.25), a narrow intense peak appeared at 1.26 h, with a maximum at 16.55 J/g h (period II). This peak was associated with the precipitation of cementitious gels, although the possible formation of secondary reaction products such as carbonates cannot be ruled out. In fact, the high alkalinity of the medium would favour carbonation (the experiments, as noted above, were conducted under laboratory conditions and not in a controlled atmosphere able to prevent exposure to CO_2), for instance, and the presence of calcium carbonate was clearly detected in the 32-min and 24-h XRD and FTIR analyses. No portlandite was detected by either technique. Calcite formation would reduce the availability of Ca^{2+} ions in the medium [55–57].

Conceptually, cement blend activation takes place as follows. When the solution comes into contact with the blend, the medium begins to be saturated with the calcium and silicon ion species dissolving out of the cement, the silicon and aluminium ion species present in the ash, and the sodium, hydroxyl and silicon ion species in the activator. The rate at which these ionic species aere solubilised affects the precipitation kinetics of the phases involved. Although due to their weaker bond strengths [58], the Ca from calcium silicates and the Al from fly ash are more soluble than the equivalent Si from these sources, the total amount of Si available is much greater overall. Consequently, the conditions favour the precipitation of a mix of gels, whose proportions depend on calcium and aluminium availability in the local environment. In other words, rather than pure gels, the hydration products consist of either an aluminium-containing (C–A–S–H-like) C–S–H gel that precipitates around the cement particles or a calcium-bearing ((N,C)–A–S–H-like) N–A–S–H gel that precipitates around the fly ash particles [44]. In the present study, gel formation was more likely to consist of only small quantities of product than result from massive precipitation, for after 24 h much of the material remained unreacted. BSEM/EDX analysis supported this hypothesis (see Fig. 7a). Here, in addition to the large amount of unreacted ash and the substantial number of C_3S particles initially present in the cement, the findings clearly showed that two gels co-precipitated: a C–A–S–H-like gel with small amounts of sodium ((N,C)–A–S–H) and a N–A–S–H gel in which the sodium was partially replaced by calcium (N,C)–A–S–H).

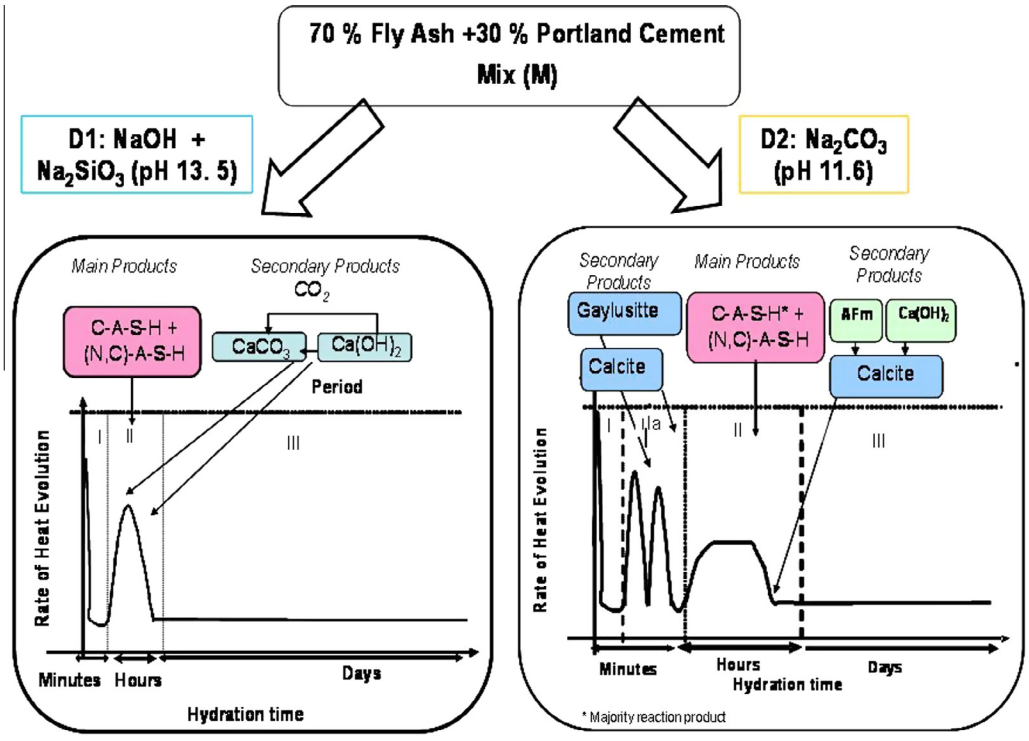

Fig. 8. Activation models for blends MD1 and MD2.

This rapidly precipitating mix of gels (a result of the high initial alkalinity in the medium) would cloak the unreacted ash and cement particles, hindering their dissolution. Consequently, both gels would subsequently precipitate via diffusion [59,60] and no peaks would be observed on the calorimetric curve after the period II signal.

Due to the use of Na_2CO_3 as an alkaline activator in MD2, this system differed in a number of ways from MD1: not only was the initial pH lower (pH = 11.3), but the solution contained CO_3^{2-}. The two calorimetric peaks recorded at 1.26 and 1.48 h in period *Ia* were associated with carbonate precipitation (a finding reported in a previous paper [61]). Finally, the heat flow curve revealed the existence of a third peak in period II, which would reflect the precipitation of the main reaction products.

XRD analyses that two types of carbonates formed: calcium carbonate and a sodium–calcium carbonate, gaylussite (period *Ia*). The latter appeared in the early stages of the reaction but soon decomposed in the aqueous phase of the mix (as Fig. 3a shows, gaylussite disappeared after 7 days).

The precipitation of the mix of cementitious gels (period II) confirmed by FTIR and BSEM/EDX (Figs. 6b and 7b) took place later than in MD1 (see Fig. 1c and e). The early precipitation of sodium–calcium carbonate would induce an initial decline in alkalinity that would result in a lower concentration of solubilised species, in particular the silicon and aluminium ionic species dissolving out of the ash. This would explain the delay in the precipitation of the cementitious gels. This decline in pH values could in turn lead to quicker hydration of the anhydrous cement phases and consequently slower ash dissolution, as suggested by the BSEM/EDX analysis. This technique showed that here the majority gel appeared to be a C–A–S–H-like product, while the proportion of (N,C)–A–S–H present was much smaller.

Gaylussite solubilisation in the medium would also lead to a rise in the dissolved sodium, calcium and carbonate ion content. The phases containing carbonate in their composition, such as AF_m, would be stabilised by the higher content of that ion [46]. The presence of hemi- and monocarboaluminates was detected on the 7-day XRD patterns. In addition, the FTIR findings confirmed $Ca(OH)_2$ formation (Fig. 3b).

By way of summary, the type of alkaline activator impacts reaction kinetics, the formation of secondary reaction products (carbonates, AF_m phases, etc.) and the proportion of the main hydration products ((N,C)–A–S–H/C–A–S–H) present. By controlling these parameters, binders could be tailored to meet specific needs.

5. Conclusions

The conclusions drawn in connection with the systems examined are set out below.

- Alkaline activators must be present to stimulate hybrid cement hydration. Overly high pH values are not needed, however. In fact, the pH of solution D2 (11.6) was considerably lower than the value for D1 (13.25). The thermodynamically stable majority product appears to be a mix of cementitious gels that forms irrespective of the activator used, although product proportions vary considerably with the activator. The use of Na_2CO_3 as an alkaline activator favours precipitation of C–A–S–H-like over (N,C)–A–S–H-like gel.
- Initial reaction kinetics differ substantially depending on the alkaline activator used. When the alkaline activator is Na_2CO_3, the precipitation of the main reaction products is retarded. The type of anion present in the activator has a significant effect on the nature of the secondary products formed. With Na_2CO_3 the formation of secondary phases such as gaylussite and AF_m type species is favoured.

Acknowledgments

This research was funded by the Spanish Ministry of Economy and Competitiveness under Project BIA 2010-17530 and supported by a Post-graduate Studies Council contract (JAE PostDoc 2011), co-funded by the Spanish National Research Council and the European Social Fund, as well as by CONSOLIDER under Project CSD 2007-00058.

References

[1] Flatt RJ, Roussel N, Cheeseman CR. Concrete: an eco material that needs to be improved. J Eur Ceram Soc 2012. http://dx.doi.org/10.1016/j.jeurceramsoc.2011.11.012.
[2] Lecomte I, Henrist C, Liégeois M, Maseri F, Rulmont A, Cloots R. (Micro)-structural comparison between geopolymers, alkali-activated slag cement and Portland cement. J Eur Ceram Soc 2006;26:3789–97.
[3] Taylor HFW. Cement chemistry. London (UK): Academic Press; 1990.
[4] Richardson IG. Nature of C–S–H in hardened cements. Cem Concr Res 1999;29:1131–47.
[5] Palomo A, Grutzeck MW, Blanco MT. Alkali-activated fly ashes: a cement for the future. Cem Concr Res 1999;29:1323–9.
[6] Shi C, Fernández-Jiménez A, Palomo A. New cements for the 21st century: the pursuit of an alternative to Portland cement. Cem Concr Res 2011;41:750–63.
[7] Yip CK, Lukey GC, van Deventer JSJ. The coexistence of geopolymeric gel and calcium silicate hydrate at the early stage of alkaline activation. Cem Conc Res 2005;35:1688–97.
[8] Alonso S, Palomo A. Calorimetric study of alkaline activation of calcium hydroxide–metakaolin solid mixtures. Cem Concr Res 2001;31:25–30.
[9] Palomo A, Fernández-Jiménez A, Kovalchuk G, Ordoñez LM, Naranjo MC. OPC–fly ash cementitious systems: study of gel binders produced during alkaline hydration. J Mater Sci 2007:2958–66.
[10] Garcia-Lodeiro I, Fernández-Jiménez A, Palomo A, Macphee DE. Effects on fresh C–S–H gels on the simultaneous addition of alkali and aluminium. Cem Concr Res 2010;40:27–32.
[11] Garcia-Lodeiro I, Fernández-Jiménez A, Palomo A, Macphee DE. Effect of calcium additions on N–A–S–H cementitious gels. J Am Ceram Soc 2010;93(7):1934–40.
[12] Garcia-Lodeiro I, Fernandez-Jimenez A, Palomo A, Macphee DE. Compatibility studies between N–A–S–H and C–A–S–H gels: study in the ternary diagram Na_2O–CaO–Al_2O_3–SiO_2–H_2O. Cem Concr Res 2011;41:923–31.
[13] Ylmén R, Wadsö L, Panas I. Insights into early hydration of Portland limestone cement from infrared spectroscopy and isothermal calorimetry. Cem Concr Res 2010;40:1541–6.
[14] ASTM C 618-94, standard specification for coal fly ash and raw or calcined natural pozzolan for use as mineral admixture in Portland cement concrete.
[15] Langan BW, Weng K, Ward MA. Effect of silica fume and fly ash on heat of hydration of Portland cement. Cem Concr Res 2002;32:1045–51.
[16] Wei FF, Grutzeck MW, Roy DM. The retarding effect of fly ash upon the hydration of cement pastes; the first 24 h. Cem Concr Res 1985;15:174–84.
[17] Way SJ, Shayan A. Early hydration of Portland cement in water and sodium hydroxide solutions: composition of solutions and nature of solid phases. Cem Concr Res 1989;19:759–69.
[18] Martinez-Ramirez S, Palomo A. OPC hydration with highly alkaline solutions. Adv Cem Res 2001;13:123–9.
[19] Martinez-Ramirez S, Palomo A. Microstructure studies on Portland cement pastes obtained in highly alkaline environments. Cem Concr Res 2001;31:1581–5.
[20] Blanco Varela MT, Martínez-Ramírez S, Gener M. Modificaciones inducidas por la adición de puzolanas naturales zeolíticas en las pastas de cemento. Mater Constr 2005;55(280):27–42.
[21] Fernandez-Jimenez A, Palomo A. Characterization of fly ash. Potential reactivity as alkaline cements. Fuel 2003;82:2259–65.
[22] Ping Yu, Kirkpatrick RJ, Poe B, McMillan PF, Cong JX. Structure of calcium silicate hydrate (C–S–H): near-, Mid-, and far-infrared spectroscopy. J Am Ceram Soc 1999;82(3):742–8.
[23] García-Lodeiro I, Fernández-Jiménez A, Blanco MT, Palomo A. FTIR study of the sol–gel synthesis of cementitious gels: C–S–H and N–A–S–H. J Sol–Gel Sci Technol 2008;45:63–72.
[24] Kovalchuk G, Fernández-Jiménez A, Palomo A. Alkali-activated fly ash: effect of thermal curing conditions on mechanical and microstructural development – part II. Fuel 2007;86:315–22.
[25] Criado M, Fernandez-Jimenez A, de la Torre AG, Aranda MAG, Palomo A. An XRD study of the effect of SiO_2/Na_2O ratio on the alkali activation of fly ash. Cem Concr Res 2007;37:671–9.
[26] Garcia-Lodeiro I, Fernández-Jiménez A, Palomo A. Variation of hybrid cement over time. Alkaline activation of fly ash-Portland cement blends. Cem Concr Res, submitted for publication.
[27] Gadsden JA. Infrared spectra of minerals and related inorganic compounds. London (England): Butterworths; 1975.
[28] Fernández-Jiménez A, Palomo A. Mid-infrared spectroscopic studies of alkali-activated fly ash structure. Microporous Mesoporous Mater 2005;86:207–14.

[29] Ylmén R, Jäglid U, Steenari BM, Panas I. Early hydration and setting of Portland cement monitored by IR, SEM and Vicat techniques. Cem Concr Res 2009;39:433–9.
[30] Vazquez Moreno T. Contribución al estudio de las reacciones de hidratación del cemento Portland por espectroscopia infraroja. Thesis (University Complutense of Madrid) (Madrid) (Spain); 1975.
[31] Garcia-Lodeiro I, Fernandez-Jimenez A, Macphee DE, Sobrados I, Sanz J. Stability of synthetic calcium silicate hydrates in presence of alkalies, aluminium and soluble silica. Transport Res Rec 2010;2142:5257.
[32] Anthony John W, Bideaux Richard A, Bladh Kenneth W, Nichols Monte C, editors. Handbook of Mineralogy, Mineralogical Society of America, Chantilly, VA 20151-1110, USA. <http://www.handbookofmineralogy.org/>.
[33] Bonavetti VL, Rahhal VF, Irassar EF. Studies on the carboaluminates formation in limestone filler-blended cements. Cem Concr Res 2001;31:853–9.
[34] Lothenbach B, Le Saout G, Gallucci E, Scrivener K. Influence of limestone on the hydration of Portland cements. Cem Concr Res 2008;38:848–60.
[35] Cassagnabére F, Mouret M, Escadeillas G. Early hydration of clinker–slag–metakaolin combination in steam curing conditions, relation with mechanical properties. Cem Concr Res 2009;39:1164–73.
[36] Snelson DG, Wild S, O'Farrel M. Heat of hydration of Portland cement–metakaolin–fly ash (PC–MK–PFA) blends. Cem Conc Res 2008;38:832–5.
[37] Meland I. Influence of condensed silica fume and fly ash on the heat evolution of cement paste. 1st international conference on the use of fly ash, silica fume, slag and natural pozzolans in concrete, vol. 2. Berlin: American Concrete Institute; 1986. p. 665–76.
[38] Kokubu M. Fly ash and fly ash cement. In: Proceedings of the fifth international symposium on the chemistry of cement. Tokyo: Cement Association of Japan; 1969. p. 75–105 [part IV].
[39] Frías M, Sánchez de Rojas MI, Cabrera J. The effect that the puzzolanic reaction of metakaolin has on the heat evolution in metakaolin–cement mortars. Cem Concr Res 2001;31:209–16.
[40] Radlinski M, Olek J. Investigation into the synergistic effects in ternary cementitious systems containing Portland cement, fly ash and silica fume. Cem Concr Com 2012;34:451–9.
[41] Bentz DP, Hansen AS, Guynn JM. Optimization of cement and fly ash particle sizes to produce sustainable concretes. Cem Concr Com 2011;33:824–31.
[42] Lothenbach B, Scrivner K, Hooton RD. Suplementay cementitious materials. Cem Concr Res 2011;41:1244–56.
[43] Damidot D, Lothenbach B, Herforts D, Glasser FP. Thermodynamics and cement science. Cem Concr Res 2011;41:679–95.
[44] Ben Haha M, de weerdt K, Lothenbach B. Quantification of the degree of reaction fly ash. Cem Concr Res 2010;40(11):1620–9.
[45] Hanehara S, Tomosawa F, Kobayakawa M, Hwang KR. Effects of water/powder ratio, mixing ratio of fly ash, and Turing temperature on pozzolnaic reaction of fly ash in cement paste. Cem Concr Res 2001;31(1):19–31.
[46] Escalante-García JI, Sharp JH. The chemical composition and microstructure of hydration products in blended cements. Cem Concr Com 2004;26:967–76.
[47] Luke K, Lachowski. Internal composition of 20-year-old fly ash and slag blended ordinary Portland cement pastes. J Am Ceram Soc 2008;91(12):4084–92.
[48] Jawed I, Skalny J. Alkalis in cement: a review, effects of alkalis on hydration and performance if Portland cement. Cem Concr Res 1978;8:37–52.
[49] Peterson VK, Neumann DA, Livingston RA. Effect of NaOH on the kinetics of tricalcium silicate hydration: a quasielastic neutron scattering study. Chem Phys Lett 2006;419:16–20.
[50] Bentz DP. Influence of alkalis on porosity percolation in hydrating cement pastes. Cem Concr Compos 2006;28:427–31.
[51] Garci Juenger MC, Jennings HM. Effects of high alkalinity on cement pastes. ACI Mat J 2001;98:251–5.
[52] Osbaeck B, Jons ES. The influence of the content and distribution of alkalis on the hydration properties of Portland cement. In: 7th International conference of cement chemistry, Paris (France); 1980. p. 135–40.
[53] Kumar A, Sant G, Patapy C, Gianocca C, Scrivener KL. The influence of sodium and potassium hydroxide on alite hydration: experiments and simulations. Cem Concr Res 2012;42:1513–23.
[54] Sant G, Kumar A, Patapy C, Gwenn Le Saout C, Scrivener K. The influence of sodium and potassium hydroxide on volume changes in cementitious materials. Cem Concr Res 2012;42:1447–55.
[55] Duchesne J, Reardon EJ. Measurement and prediction of portlandite solubility in alkaline solutions. Cem Concr Res 1995;25:1043–53.
[56] Fratini N. Solubility of calcium hydroxide in presence of potassium and sodium hydroxides. Ann Chim Appl 1949;39:616–22.
[57] Diamond S. The status of calcium in pore solution of mature hardened Portland cement. Il Cemento 1977;74:149–56.
[58] Iler RK. The chemistry of silica. New York (USA): Wiley; 1955.
[59] Verbeck GJ, Helmuth RH. Structure and physical properties of cement pastes. In: 5th Int Cong On the Chem Cem, Tokyo, vol. III; 1968. p 1–32.
[60] Fernández-Jiménez A, Palomo A, Criado M. Microstructure development of alkali-activated fly ash cement: a descriptive model. Cem Concr Res 2005;35(6):1204–9.
[61] Caijun Shi C, Day RL. A calorimetric study of early hydration of alkali–slag cements. Cem Concr Res 1995;25:1333–46.